Short communication

Hydrogen storage in carbon fibers activated with supercritical CO_2: Models and the importance of porosity

F. Salvador*, M.J. Sánchez-Montero, J. Montero, C. Izquierdo

Dpto. Química Física, Plaza de la Merced s/n, Facultad de Ciencias Químicas, Universidad de Salamanca, 37006 Salamanca, Spain

ABSTRACT

In this work we studied the adsorption of H_2 at 77 K and 0.0–0.12 MPa onto carbon fibers activated with supercritical CO_2 (ACFs) and with different burn-offs (10–53%). The highest amount of H_2 stored was 2.45 wt% in an ACF with a burn-off of 51% at 0.12 MPa. The measured isotherms were analyzed using an equilibrium model derived by analogy with a multiple-site Langmuir-type adsorption model. The different equilibria correspond to adsorption in pores of different sizes. The experimental results fitted a model with two different adsorption sites satisfactorily, allowing such sites to be related to the microporous structure of the ACFs. Thus, a high-energy adsorbent–adsorbate interaction site, associated with very small micropores, accessible only to very small molecules such as H_2, and another lower-energy site associated with larger pores can be proposed. The model also predicts the adsorption behavior under equilibrium conditions at higher pressures, allowing the maximum adsorption capacity of the ACFs to be determined. The results show that the ACFs adsorb most of the H_2 molecules at low equilibrium pressures, and that they become almost saturated at pressures around 1.0 MPa. The maximum H_2 storage capacity in these ACFs lies between 1.50 and 3.15 wt%.

© 2009 Elsevier B.V. All rights reserved.

1. Introduction

In recent years there has been increasing interest in finding a method for storing H_2 that will allow its use on vehicles. In this sense, the process of adsorption onto carbonaceous materials seems to be one of the most promising [1,2]. Research in this field is vigorous; some authors have focused on seeking materials and preparation conditions with a view to achieving maximum storage capacity, while others have investigated the relationship between the textural characteristics of the adsorbent materials and their storage capacity. Concerning this latter, there is some controversy in the sense that some investigators have reported a linear dependence of the specific surface area, S_{BET}, of the adsorbent on the adsorption capacity [3–5]. Others, in contrast, have proposed that it is the narrowest microporosity that is tightly related to the capacity to adsorb H_2 [6–9].

The aim of this work was to focus on a less known aspect; namely the search for an adsorption model that would describe the experimental results in a satisfactory way. The study was carried out with ACFs prepared using a novel procedure of physical activation with supercritical CO_2.

2. Experimental

As starting material, a Novoloid phenolic textile fiber supplied by Kynol and carbonized at 750 °C in an inert atmosphere of nitrogen was employed. The ACFs were prepared by physical activation of the carbonized fiber using supercritical CO_2 ($SCCO_2$) as the activating agent at 11 MPa and different temperatures: 750, 775 and 800 °C. These conditions were kept for several time intervals in order to achieve different burn-off degrees (10–53%). A more detailed description of the experimental details concerning the preparation of the ACFs can be found in previous reports [10,11]. Burn-off was determined from the loss of mass undergone by the carbon fibers during the activation process. The nomenclature used to refer to the different series of ACFs is as follows: the activation temperature, followed by "ACF" and finally the percentage of burn-off. Changes in the porosity of the carbonized fibers produced by the different experimental conditions were analyzed from the physical adsorption isotherms of N_2 at 77 K, measured on an automatic volumetric adsorption apparatus, ASAP 2010, from Micromeritics.

The parameters determined were as follows: (i) specific surface area, S_{BET}, calculated by applying the BET equation [12] to the N_2 adsorption isotherm at 77 K; (ii) micropore volume deduced from application of the Dubinin–Raduskhevich equation [13] to the adsorption isotherms, $V_0(N_2)$; (iii) mean pore width, L_{SB}, deduced from the Characteristic Energy by application of the Stoeckli and Ballerini equation [14].

* Corresponding author. Tel.: +34 932294478; fax: +34 923294574.
E-mail address: salvador@usal.es (F. Salvador).

The H_2 storage capacity was determined from the adsorption–desorption isotherms of H_2 at 77 K and at pressures of 0–0.12 MPa, using a Micromeritics Tristar device.

3. Results

3.1. Textural characteristics

The textural characteristics of the carbonized fiber and of the different ACFs are shown in Table 1, together with the corresponding percentage of H_2 adsorbed and the average density of hydrogen adsorbed at a pressure of 0.12 MPa and a temperature of 77 K. Calculation of this density was performed based on the amount of H_2 adsorbed and the micropore volume, $V_0(N_2)$, assuming that all the H_2 had been homogeneously adsorbed in the micropore. As the starting material, the carbonized fiber already showed very high values of the textural parameters. This indicates the presence of a large incipient microporosity. For the three series of ACFs prepared, S_{BET} and $V_0(N_2)$ increased with the burn-off, reaching maximum values of $1904\,m^2\,g^{-1}$ and $0.73\,cm^3\,g^{-1}$ for the 775ACF51 sample; i.e., typical of highly microporous materials. This evolution of the porosity with activation may have been favored by the $SCCO_2$ because it penetrates the whole microporous structure of the carbonized fiber more easily, thanks to the pressure applied [11]. Thus, a highly uniform activation must have occurred, with a widening of the micropores, since the start of activation. The ACFs selected in this work covered a broad range of micropore sizes: from 0.49 nm to 1.19 nm.

In Table 1 it may also be seen that the ACFs rapidly increased the amount of H_2 adsorbed when the burn-off was increased and at the same time the density of the H_2 adsorbed decreased.

Fig. 1 shows the evolution of the amount of H_2 adsorbed *versus* $V_0(N_2)$. All the ACFs, regardless of the experimental conditions used in their preparation, increased the amount of H_2 adsorbed as $V_0(N_2)$ increased. A similar kind of behavior was found upon correlating the amount of H_2 adsorbed with the S_{BET}. Different authors have reported linear relationships between the adsorption capacity and some of these textural parameters [7]. However, as seen in Fig. 1 for these fibers the correlation is not linear, pointing to a less marked increase in the H_2 adsorbed for the highest $V_0(N_2)$ values.

Fig. 2 shows the density of hydrogen adsorbed at a pressure of 0.12 MPa against mean micropore width. It may be seen that density increased rapidly with the decrease in mean micropore width. Sample 775ACF11, with a pore width of 0.51 nm, is the one showing the highest density: $0.053\,g\,cm^{-3}$. This density is close to that of liquid H_2 at 1 atm and 20.3 K ($0.0708\,g\,cm^{-3}$), pointing to the strong interaction between the surface of the ACF and the H_2. Theoretical studies [15–17] have shown that the maximum packing of H_2
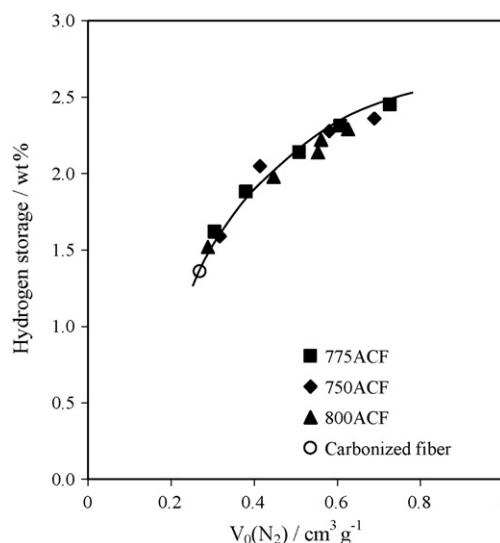

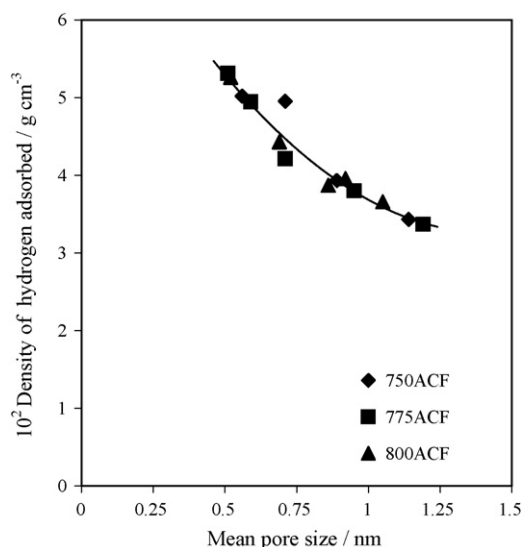**Fig. 1.** Evolution of the H_2 stored with micropore volume.

Fig. 2. Variation in the density of H_2 adsorbed with micropore width.

molecules is achieved in pores whose width ranges between 0.36 and 0.56 nm. This very high storage density, $0.053\,g\,cm^{-3}$, which is achieved by having the H_2 adsorbed in the pores at an equilibrium pressure of 0.12 MPa, would be equivalent to having the H_2 stored in

Table 1
H_2 adsorption and textural parameters of the ACFs.

Sample	S_{BET} $(m^2\,g^{-1})$	$V_0(N_2)$ $(cm^3\,g^{-1})$	$L_{(S-B)}$ (nm)	H_2 storaged to 0.12 MPa (wt%)	$\rho_{H_2\ adsorbed}$ $(g\,cm^{-3})$
Carbonized fiber	499	0.27	0.49	1.36	0.050
750ACF12	806	0.32	0.56	1.59	0.050
750ACF24	1054	0.41	0.71	2.05	0.049
750ACF39	1487	0.58	0.89	2.28	0.039
750ACF53	1804	0.69	1.14	2.36	0.034
775ACF11	777	0.30	0.51	1.62	0.053
775ACF20	966	0.38	0.59	1.88	0.049
775ACF30	1286	0.51	0.76	2.14	0.042
775ACF43	1560	0.61	0.95	2.31	0.038
775ACF51	1904	0.73	1.19	2.45	0.034
800ACF10	735	0.29	0.52	1.52	0.052
800ACF24	1133	0.45	0.69	1.98	0.044
800ACF35	1401	0.55	0.86	2.14	0.039
800ACF43	1459	0.56	0.92	2.22	0.040
800ACF51	1638	0.63	1.05	2.29	0.036

a deposit at a pressure of 22.8 MPa. Of all the fibers prepared, sample 775ACF51 was the one that adsorbed the most H_2 (2.45 wt%). However, it was not the sample with the greatest H_2 packing but the one with the greatest $V_0(N_2)$ and S_{BET}. This value for the H_2 adsorption capacity is in agreement with those reported by other authors [18,6,19]. Currently, amounts of adsorbed H_2 greater than 5 wt% can be reached at 77 K, but at high pressures. The greatest adsorption capacities tend to correspond to chemically activated and super-activated carbons [20].

Moreover, if the volume occupied by the fiber (0.8 g cm^{-3}) is taken into account, simple calculations show that the H_2 stored per unit volume at the equilibrium pressure of 0.12 MPa in the 775ACF51 sample would be equivalent to having the H_2 stored without adsorbent at a pressure of 6.1 MPa.

All these findings highlight the advantage of using an adsorbent to store hydrogen and suggest that there is a close relationship between the microporosity of the fibers and their capacity to adsorb H_2.

3.2. Adsorption isotherms

We obtained the adsorption–desorption isotherms of H_2 at 77 K from 0.0 to 0.12 MPa for all the ACFs prepared and the carbonized fiber. Fig. 3 shows the isotherms plotted on the linear and logarithmic scales of the 775ACF series. The adsorption isotherms are in agreement with the desorption isotherms and no hysteresis was observed, pointing to the reversibility of the adsorption and that it is physical.

All the isotherms have similar shapes: Type I according to the IUPAC classification. The carbonized fiber adsorbed a large amount of H_2. For pressures lower than 3 kPa, the amount of H_2 adsorbed decreased slightly with the increase in burn-off. However, for pressures higher than this the trend was reversed, and the amount of H_2 adsorbed increased with burn-off in a more marked fashion. This kind of behavior occurs because the smaller micropores of the carbonized fiber decrease progressively with burn-off while the larger micropores increase in number [11].

This shape of the isotherms has been confirmed by different authors for the adsorption of H_2 on different carbonaceous materials, suggesting that they can be satisfactorily fitted to the Langmuir equation [5,21]. Fig. 4 shows the fitting to that equation for the isotherms corresponding to two fibers with different burn-offs. In all cases, this Langmuir model cannot fit the experimental data well, showing that the ACF/H_2 adsorption system is complex.

3.3. Two-site adsorption model

A much more precise correlation was obtained when the experimental results were fitted to a Langmuir model with two energetically different adsorption sites:

$$n = \frac{n_1 K_1 p}{1 + K_1 p} + \frac{n_2 K_2 p}{1 + K_2 p}$$

where n is the amount of H_2 adsorbed at equilibrium per unit mass of adsorbent at the equilibrium pressure p; n_i is the maximum amount of H_2 adsorbed at site i, which is achieved when the adsorption site is filled, and K_i is the affinity constant or Langmuir constant, which provides information about the strength with which the molecule of adsorbate is bound to site i. All the isotherms are very precisely correlated with this model. Fig. 4 shows this correlation together with the contribution of each site for two ACFs with different burn-offs. In all cases, site 1 was rapidly saturated, even at low equilibrium pressures and low burn-offs. Site 2, except for very low pressures, adsorbed more H_2 than site 1 and was only saturated at greater pressures.

Table 2 shows the values of the parameters n_i and K_i for the carbonized fiber and all the ACFs prepared. Site 1 is saturated and retains almost the same amount of H_2 for any burn-off, although the strength of adsorption is very high and progressively declines with burn-off. Also, the maximum amount of H_2 that can be retained by site 2 is greater than that of site 1 and increases with burn-off. Nevertheless, the strength of H_2 adsorption at this site is much smaller than that seen for site 1 and also decreases as burn-off increases. This behavior of sites 1 and 2 suggests that site 1 may be associated with very small micropores and site 2 with larger ones. The high values of K_1 and the low values of K_2 clearly indicate that sites 1 and 2 are very different and may be identified with very small micropores, where the adsorbent–adsorbate interactions are very strong, and larger micropores, where such interactions are small respectively.

From the four parameters it is possible to predict the adsorption capacity for different equilibrium pressures. The sum of n_1 and n_2 provides the maximum adsorption capacity of the fiber (Table 2). Table 2 also shows the amounts of H_2 adsorbed by all the ACFs extrapolated to the equilibrium pressure of 1.0 MPa, and it may be seen that for that pressure the ACFs are very close to saturation. These findings show that at low pressures (>0.12 MPa) the adsorption capacity of the ACFs increases rapidly with temperature. However, at higher pressures the increase is much less
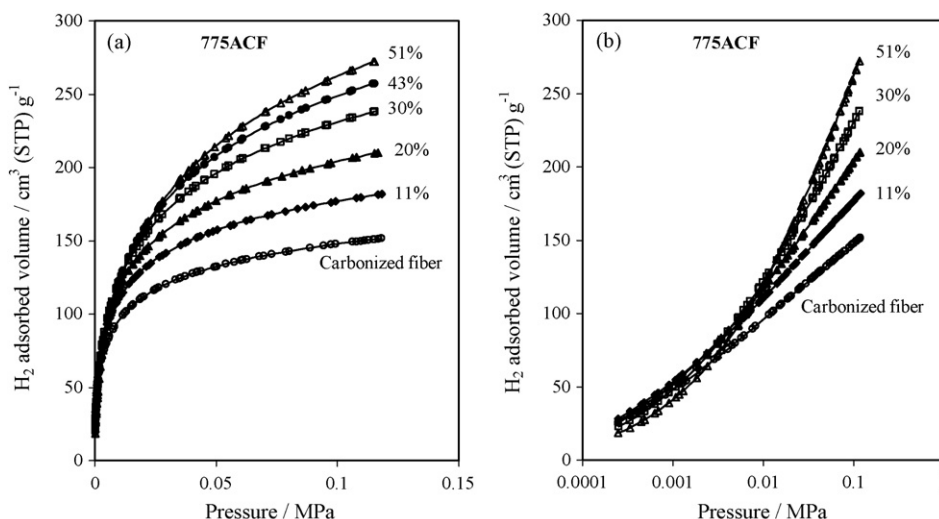

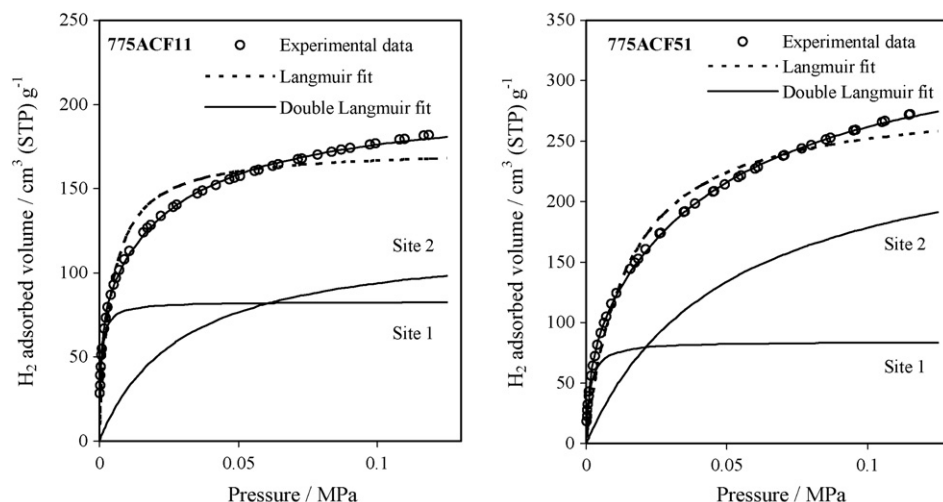**Fig. 3.** H_2 adsorption isotherms at 77 K: (a) linear form; (b) logarithmic form.

Fig. 4. Fitting of two isotherms to the Langmuir equation and to the Langmuir double equation with the contribution of each of the sites.

Table 2
Parameters of the Langmuir double equation and maximum amount of H_2 storage.

Sample	n_1 (cm³ (STP) H_2 g⁻¹ fiber)	K_1 (MPa⁻¹)	n_2 (cm³ (STP) H_2 g⁻¹ fiber)	K_2 (MPa⁻¹)	Maximum H_2 storage to 1 MPa (wt%)	Predicted maximum H_2 storage (wt%)
Carbonized fiber	73.6	1666.3	94.7	36.0	1.48	1.50
750ACF12	80.9	1362.4	121.6	32.1	1.78	1.81
750ACF24	83.8	1088.2	191.2	26.2	2.40	2.46
750ACF39	88.3	848.3	233.5	20.6	2.78	2.87
750ACF51	79.4	782.1	259.2	20.5	2.91	3.03
775ACF11	82.8	1590.7	121.1	34.4	1.79	1.82
775ACF20	86.9	1295.1	157.7	28.7	2.14	2.19
775ACF30	89.2	978.2	199.6	24.6	2.51	2.58
775ACF43	90.1	789.8	231.9	21.9	2.78	2.88
775ACF51	84.4	740.8	267.3	20.0	3.03	3.15
800ACF10	76.6	1685.7	112.4	38.1	1.66	1.69
800ACF24	86.4	1172.7	174.6	27.7	2.28	2.34
800ACF35	90.1	872.5	201.6	23.7	2.53	2.61
800ACF43	86.1	724.8	226.9	21.0	2.70	2.80
800ACF51	81.9	814.8	240.8	21.6	2.79	2.88

pronounced, such that at 1.0–1.5 MPa the fibers are almost completely saturated. Thus, for example, the 775AC51 fiber adsorbed 2.45 wt% at 0.12 MPa and 3.03 wt% at 1.0 MPa, its maximum adsorption capacity being 3.15 wt%. Fig. 5 shows the evolution of K_2 with

the mean pore width for the three series of activated fibers and the carbonized fiber. Again, it may be seen that the value of K_2 is independent of the temperature at which the samples were prepared and that it decreases sharply with pore width. This decrease
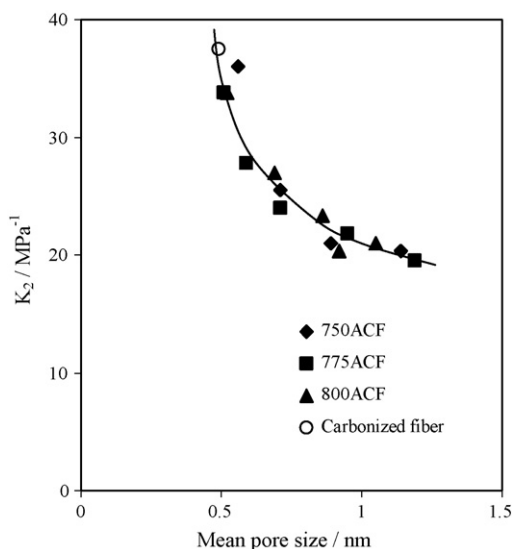

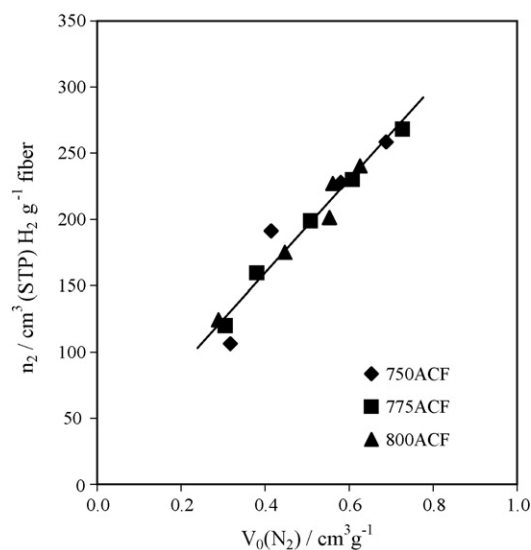**Fig. 5.** Variation in the K_2 parameter with micropore width.

Fig. 6. Dependence of the maximum amount of H_2 retained at site 2 on micropore volume.

is similar to the variation in the density of the H_2 adsorbed with the pore size shown in Fig. 2. This behavior was expected because when the pores are very narrow the adsorbent–adsorbate interactions are very strong and the packing density is very high. However, when the pores are widened, the packing density declines sharply, as do the adsorbent–adsorbate interactions [15].

Additionally, the amount of H_2 adsorbed in site 2, n_2, shows an almost linear increase with the micropore volume, $V_0(N_2)$, Fig. 6. Nevertheless, the amount of H_2 retained in site 1, n_1, remains almost constant for all burn-offs, such that it is not directly related to the evolution of the different textural parameters.

All the above findings suggest that the carbonized fiber contains very small micropores that are hardly widened at all during the activation process since the activating agent (CO_2) is unable to penetrate them. Furthermore, neither they are detected by the N_2 used in the textural characterization, although they are accessible to H_2 thanks to the small size of this molecule. These micropores would thus be identified with site 1 and the other larger ones with site 2.

4. Conclusions

Three series of ACFs prepared at 750, 775 and 800 °C have been used to study H_2 adsorption at 77 K in the 0.0–0.12 MPa pressure range. In all three series the amounts of H_2 adsorbed increased steadily with the burn-off and $V_0(N_2)$ volume, and was independent of the activation temperature.

The maximum amount of H_2 stored at 0.12 MPa was 2.45 wt% for the 775AC51 fiber. This fiber has the highest S_{BET} and $V_0(N_2)$, and yet it shows the lowest parking density of H_2 molecules (0.034 g cm^{-3}). This density is quite high taking into account the density of liquid H_2 (0.0708 g cm^{-3}).

The Langmuir adsorption model with two sites satisfactorily reproduces the behavior of the adsorption of H_2 in these ACFs. The site with the greatest energy adsorbed only a small amount of H_2, although with great strength, and became saturated at very low pressures; around 0.12 MPa. This site would be associated with very small micropores, not accessible to N_2 molecules. In contrast, the lower-energy site would retain much more H_2, although only weakly, becoming saturated at higher pressures. The model also provided information about the maximum amount of H_2 that can be stored in the ACFs and allows the amount of adsorbed H_2 to be extrapolated to higher pressures. For all the ACFs assayed, H_2 was mainly adsorbed in the pressure range tested (0.0–0.12 MPa), the materials becoming saturated at pressures around 1.0 MPa.

References

[1] A.C. Dillon, M.J. Heben, Applied Physics A: Materials Science and Processing 72 (2001) 133–142.
[2] F. Lamari Darkrim, P. Malbrunot, G.P. Tartaglia, International Journal of Hydrogen Energy 27 (2002) 193–202.
[3] M.G. Nijkamp, J.E.M.J. Raaymakers, A.J. van Dillen, K.P. de Jong, Applied Physics A 72 (2001) 619–623.
[4] R. Ströbel, L. Jörissen, T. Schliermann, V. Trapp, W. Schütz, K. Bohmhammel, G. Wolf, J. Garche, Journal of Power Sources 84 (1999) 221–224.
[5] B. Panella, M. Hirscher, S. Roth, Carbon 43 (2005) 2209–2214.
[6] K. Mark Thomas, Catalysis Today 120 (2007) 389–398.
[7] L.L. Vasiliev, L.E. Kanonchik, A.G. Kulakov, D.A. Mishkinis, A.M. Safonova, N.K. Luneva, International Journal of Hydrogen Energy 32 (18) (2007) 5015–5025.
[8] N. Texier-Mandoki, J. Dentzer, T. Piquero, S. Saadallah, P. David, C. Vix-Guterl, Carbon 42 (2004) 2735–2777.
[9] W.-C. Takahashi, K. Matsuo, Y. Hattori, M. Kumagai, S. Ishiyama, K. Kaneko, S. Iijima, International Journal of Hydrogen Energy 32 (13) (2007) 2504–2512.
[10] F. Salvador, M.J. Sánchez Montero, C. Izquierdo, Journal of Physical Chemistry C 111 (2007) 14011–14020.
[11] M.J. Sánchez Montero, F. Salvador, C. Izquierdo, Journal of Physical Chemistry C 112 (37) (2008) 4991–4999.
[12] F. Salvador, C. Sánchez-Jiménez, M.J. Sánchez-Montero, A. Salvador, Studies in Surface Science and Catalysis 144 (2002) 379–386.
[13] M.M. Dubinin, Chemistry Reviews 60 (2) (1960) 235–241.
[14] F. Stoeckli, L. Ballerini, Fuel 70 (1991) 557.
[15] M. Rzepka, P. Lamp, M.A. de la Casa-Lillo, Journal of Physical Chemistry B 102 (1998) 10894.
[16] Q. Wang, J.K. Johnson, Journal of Chemical Physics 110 (1999) 577.
[17] M.A. de la Casa-Lillo, F. Lamari-Darkrim, D. Cazorla-Amorós, A. Linares-Solano, Journal of Physical Chemistry B 106 (2002) 10930–10934.
[18] M. Jordá-Beneyto, F. Suarez-García, D. Lozano-Castelló, D. Cazorla-Amorós, A. Linares-Solano, Carbon 45 (2007) 293–303.
[19] M.Z. Figueroa-Torres, A. Robau-Sánchez, L. de la Torre-Sáenz, A. Aguilar-Elguézabal, Microporous and Mesoporous Materials 98 (2007) 89–93.
[20] W.-C. Xu, K. Takahashi, Y. Matsuo, Y. Hattori, M. Kumagai, S. Ishiyama, K. Kaneko, S. Iijima, International Journal of Hydrogen Energy 37 (2007) 2504–2512.
[21] X.B. Zhao, B. Xiao, A.J. Fletcher, K.M. Thomas, Journal of Physical Chemistry B 109 (2005) 8880–8888.